Dynamic Determination of Pile Capacity

By Frank Rausche,[1] M. ASCE, George G. Goble,[2] M. ASCE, and Garland E. Likins, Jr.[3]

Abstract: A method is presented for determining the axial static pile capacity from dynamic measurements of force and acceleration made under the impact of a large hammer. The basic equation for calculation of the forces resisting pile penetration is derived. The limitations of the basic resistance equation are discussed and illustrative examples of field measurements are given. With the availability of this derivation, it is possible to prove that the Case Pile Wave Analysis Program (CAPWAP) resistance force distribution is unique. Using the assumption that the resistance to penetration can be divided into static and dynamic parts, an expression is developed for calculating the dynamic resistance to penetration. The resulting method requires the selection of a "damping" constant which is shown empirically, to relate to soil size distribution. A correlation of Case Method capacity and the capacity observed in static load tests is given for 69 statically tested piles that were also tested dynamically.

Introduction

The idea of using measurements made during pile driving to estimate pile capacity is an old one. Since pile driving causes failure of the soil, it is logical to use measurements made during driving to predict pile capacity. This was the basis of all of the dynamic pile formulas that have been used for more than 100 yr. Since only the simplest measurements were possible when the formulas were developed (permanent set per hammer blow), it was natural to use an energy approach. Unsatisfactory results have been obtained because of the very poor representation of all elements of the system that was necessary in this approach. In the intervening period, considerable effort has been devoted to modifying the dynamic formulas to produce better results. There is no indication that improvements have been obtained with the more advanced formulas.

With the developments in electronics made during the past 20 yr, it is now practical to measure parameters other than pile set, and these measurements have made improved analysis methods possible. By the 1930's, force measurements were already being made at the pile head during driving (2). In an extensive pile testing program conducted by the Michigan Highway Department in 1961, both force and acceleration were measured in the driving system (10). Beginning in 1964, a research program at Case Institute of Technology (now Case Western Reserve University) collected large volumes of force and acceleration measure-

[1]Pres., Goble, Rausche, Likins and Assoc., Inc., 4423 Emery Industrial Parkway, Warrensville Heights, Ohio 44128.

[2]Prof., Dept. of Civ., Environmental and Architectural Engrg., Univ. of Colorado, Boulder, Colo. 80309.

[3]Pres., Pile Dynamics, Inc., 4423 Emery Industrial Parkway, Warrensville Heights, Ohio 44128.

Note.—Discussion open until August 1, 1985. To extend the closing date one month, a written request must be filed with the ASCE Manager of Journals. The manuscript for this paper was submitted for review and possible publication on February 8, 1984. This paper is part of the *Journal of Geotechnical Engineering*, Vol. 111, No. 3, March, 1985. ©ASCE, ISSN 0733-9410/85/0003-0367/$01.00. Paper No. 19551.

ments on test piles during driving or, more frequently, during restrike (4,5,6,7). This project was active for several years, and during this time, the capability to make these measurements on a routine basis and then process them automatically was developed (3,14) to a point of practical application to routine piling projects. [Measurement and processing equipment have been thoroughly reviewed elsewhere (9,13) and will not be repeated here.]

The project developed means of analysis to determine wave equation soil parameters active during impact using a program known as the Case Pile Wave Analysis Program (CAPWAP) (15). The CAPWAP analysis requires a substantial computational effort and, therefore, is usually performed in the office with more extensive computer hardware. Analysis requires about two hr of engineering time per hammer blow on a microcomputer in an interactive environment.

Several simplified methods of analysis using closed form solutions of the one-dimensional wave propagation theory were also developed using empirical correlations to static pile test results. These solutions can be obtained in real time for each hammer blow. These methods were improved over a period of time and they have become known as the Case Method. At the completion of the Case project, a rational analysis method had been developed (4).

The purpose of this paper is to present the derivation of the Case Method, and to discuss the assumptions contained in the governing equations. Sources of error are identified, and means of avoiding or correcting the difficulties are considered. Using the Case Method derivation, it is easy to prove the theoretical uniqueness of CAPWAP. Since questions have been raised on this point (16), it is relevant to present the proof here.

Wave Mechanics

When a slender rod (or a pile) is subjected to a suddenly applied axial force, a stress wave that travels away from the point of force application is induced. This problem was solved in the 19th century for the case of linear elastic materials and rods of uniform cross section (18). Only axial stresses were assumed to exist, but, subsequently, more complex cases have been studied. It has been shown that as long as no reflections arrive at the point under consideration (or where measurements are being made), the force in the pile is proportional to the velocity of particle motion. This relationship can be stated

$$v(t) = \frac{c}{EA} F(t) \qquad (1)$$

in which v = velocity of particle motion (downward positive) at the point under consideration; and F = the force (compression positive) at the same point, both given as a function of time. Parameter c = velocity of propagation of the stress wave; E = modulus of elasticity of the material; and A = rod cross-sectional area. With ρ = mass density of the pile material, the wave speed is

$$c = \sqrt{\frac{E}{\rho}} \quad \ldots\ldots (2)$$

For compression waves, the particle velocity is in the direction of the propagation; for tension waves, the particle velocity is opposite to the direction of wave propagation and a negative sign is then included in Eq. 1. It has been shown that a stress wave, propagating in a completely free rod, is unchanged in magnitude during propagation, provided that internal damping is small enough to be neglected. Thus, a stress state—given as a function of position along the rod at some instant in time—will be of the same magnitude and shape at a later instant in time, but it will be located at another position in the rod.

If a rod (or a pile) of length L is completely free, then at time $t = L/c$, after the stress is induced at the pile head, the stress wave arrives at the pile toe. For a free boundary condition (no axial forces act on the pile toe), a stress wave of identical magnitude, but opposite sign, is reflected back toward the pile head. The velocities in the 2 waves superimpose during reflection, causing the pile end velocity to double. The proportionality between force and velocity, given in Eq. 1, for the pile head, will hold until the reflected wave arrives at the pile head. In the opposite extreme, for a rod with a fixed toe, the reflected force is of the same sign and magnitude as the initial wave. As the input and reflected waves superimpose theoretically, the force can double during reflection at the fixed end. For a detailed review of wave propagation, see Ref. 18.

For a pile of finite length with free ends, the velocity at the pile head is given by

$$v_T^o(t) = \frac{c}{EA}\left[F_T(t) + 2F_T\left(t - \frac{2L}{c}\right) + 2F_T\left(t - \frac{4L}{c}\right) + \ldots\right] \quad \ldots\ldots (3)$$

in which subscript T refers to a point at the pile head. This velocity is referred to as a free pile solution since no resistance forces are present; and, therefore, the superscript o is used. In Eq. 3, the reflection condition at the head is assumed to be free since a force boundary condition is prescribed. When the tension wave reflected from the toe arrives at the head, the velocity doubles in order that the equilibrium is satisfied. Fig. 1 shows this relationship for a step function applied pile head force, F_{Ta}, that remains constant in time.

Resistance forces create a more complex wave behavior since, in general, they act at some intermediate location. Consider the effect of a suddenly applied, upward acting force at a location some distance, x, from the pile head on a pile with a free toe. The action of such a force will induce 2 stress waves in the pile, one traveling upward and one downward. The upward traveling wave will be a compression wave and the downward traveling wave, a tension wave. The particle velocities of each of these waves are

$$v_R(t) = \frac{1}{2}\frac{c}{EA}R(t) \quad \ldots\ldots (4)$$

in which $R(t)$ = the force acting at a particular intermediate location; and subscript R refers to the wave effect being generated from a resistance

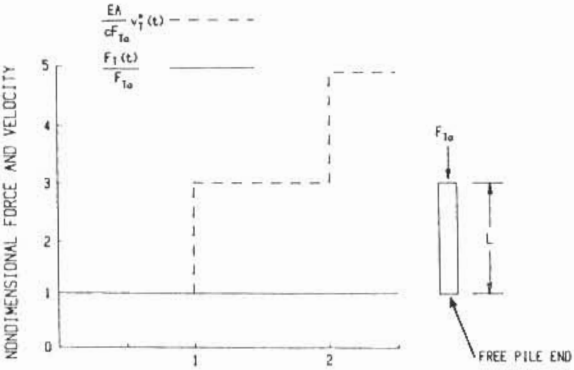

FIG. 1.—Free Pile Top Force and Velocity under Action of Suddenly Applied Constant Force

force. Thus, a compression wave having a force of one-half the resistance force will be directed to the head. The other half of the effect of force $R(t)$ appears as a tension wave traveling to the pile toe where it reflects back up the pile. Since it changes sign at the free end, it reflects as a compression wave. The total force, $R(t)$, is transmitted to the pile head, but the 2 parts arrive at different times.

If the assumption is made that forces in the form of soil resistances are concentrated at n locations, x_i, $i = 1, 2, \ldots, n$ (x is measured from the pile head) with magnitudes R_i, then

$$R_i(t) = R_i H\left(t - \frac{x_i}{c}\right) \quad \text{(5)}$$

in which $H(t - a)$ = the Heaviside step function which is zero for $t < a$, and unity for $t \geq a$. If $t = 0$ is the time of impact, this resistance law implies that the resistance forces act only after the impact wave has reached their respective locations. The effect of the upward traveling wave caused by $R_i(t)$ is felt at the pile head with a delay, x_i/c, from the time of its initiation, and the downward traveling portion with a delay of $(2L - x_i)/c$. Thus, the first effect of the downward traveling wave arrives at the top together with the tip reflection of the impact wave. For all time, the change of the particle velocity at the pile head due to the upward traveling portion caused by $R_i(t)$ is

$$v_{Ti}^{u}(t) = -\frac{c}{EA} R_i\left[H\left(t - \frac{2x_i}{c}\right) + H\left(t - \frac{2x_i + 2L}{c}\right) + H\left(t - \frac{2x_i + 4L}{c}\right) + \ldots\right] \quad \text{(6a)}$$

The downward traveling portion of the wave causes a velocity change of

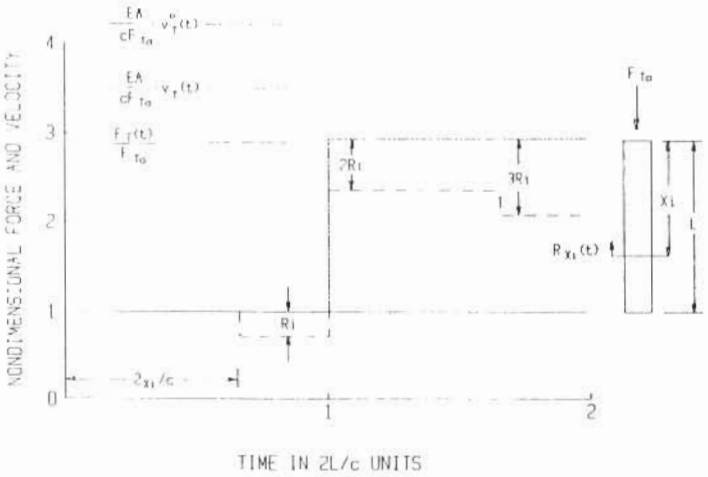

FIG. 2.—Pile Top Force and Velocity for Suddenly Applied Constant Force with One Side Resistance Force

$$v_T^d(t) = -\frac{c}{EA} R_i \left[H\left(t - \frac{2L}{c}\right) + H\left(t - \frac{4L}{c}\right) + \ldots \right] \quad \ldots\ldots\ldots\ldots\ldots\ldots (6b)$$

Finally, the net velocity can be obtained by superimposing the velocities given by Eqs. 3 and 6*a–b*.

$$v_T(t) = \frac{c}{EA} \left\{ F_T(t) + 2 \sum_{j=1}^{m} F_T\left(t - \frac{j2L}{c}\right) - \sum_{i=1}^{n} R_i \left[H\left(t - \frac{2x_i}{c}\right) \right.\right.$$

$$\left.\left. + \sum_{j=1}^{m} H\left(t - \frac{2x_i + j2L}{c}\right) + \sum_{j=1}^{m} H\left(t - \frac{j2L}{c}\right) \right] \right\} \quad \ldots\ldots\ldots\ldots\ldots\ldots\ldots\ldots (7)$$

in which m = the number of $2L/c$ time intervals after impact. For a single resistance force, $R_i(t)$, Fig. 2 gives an example which also includes the pile force $F_T(t)$ of Fig. 1. Note that the particle velocity at the pile head, due to the resistance only, is the sum of Eqs. 6*a–b*, or the difference between the $v_T^0(t)$ line, i.e., the free solution of Eq. 3 and the $v_T(t)$ line. Thus

$$v_R^0(t) - v_T(t) = \frac{c}{EA} \sum_{i=1}^{n} R_i \left[2m + H\left(t - \frac{2x_i + 2mL}{c}\right) \right] \quad \ldots\ldots\ldots\ldots\ldots\ldots (8)$$

in which m = the number of completed $2L/c$ time intervals.

If the measured velocity, $v_m(t)$, at any time, t^*, is considered in Eq. 7, and the measured velocity at a time, $2L/c$, later is subtracted, then in terms of the measured force, $F_m(t)$:

$$\frac{EA}{c} \left[v_m(t^*) - v_m\left(t^* + \frac{2L}{c}\right) \right] = F_m(t^*) + 2 \sum_{j=1}^{m} F_m\left(t^* - \frac{j2L}{c}\right) - F_m\left(t^* + \frac{2L}{c}\right)$$

$$- 2 \sum_{j=1}^{m+1} F_m\left(t^* + \frac{2L}{c} - \frac{j2L}{c}\right) - \sum_{i=1}^{n} R_i \left[2m + H\left(t^* - \frac{2x_i + 2mL}{c}\right)\right.$$

$$\left. - 2(m+1) - H\left(t^* + \frac{2L}{c} - \frac{2x_i + 2(m+1)L}{c}\right)\right] \quad \ldots\ldots\ldots\ldots\ldots\ldots\ldots\ldots (9)$$

Since the arguments of the Heaviside function terms both have the same value, their effects cancel and the expression simplifies to

$$\frac{EA}{c}\left[v_m(t^*) - v_m\left(t^* + \frac{2L}{c}\right)\right] = -F_m(t^*) - F_m\left(t^* + \frac{2L}{c}\right)$$

$$- \sum_{i=1}^{n} R_i[2m - 2(m+1)] \quad \ldots\ldots\ldots\ldots\ldots\ldots\ldots\ldots\ldots\ldots\ldots\ldots\ldots\ldots\ldots\ldots (10)$$

Now if all of the values of R_i are summed, they can be denoted

$$R(t^*) = \sum_{i=1}^{n} R_i \quad \ldots\ldots\ldots\ldots\ldots\ldots\ldots\ldots\ldots\ldots\ldots\ldots\ldots\ldots\ldots\ldots\ldots\ldots\ldots\ldots\ldots\ldots (11)$$

The total resistance can then be given as a function of the time, t^*, when computation begins.

$$R(t^*) = \frac{1}{2}\left[F_m(t^*) + F_m\left(t^* + \frac{2L}{c}\right)\right] + \frac{EA}{2c}\left[v_m(t^*) - v_m\left(t^* + \frac{2L}{c}\right)\right] \quad \ldots\ldots (12)$$

For a uniform pile

$$\frac{EA}{c} = \frac{Mc}{L} \quad \ldots\ldots\ldots\ldots\ldots\ldots\ldots\ldots\ldots\ldots\ldots\ldots\ldots\ldots\ldots\ldots\ldots\ldots\ldots\ldots\ldots\ldots\ldots\ldots (13)$$

in which M = the total mass of a pile of length L. Thus, Eq. 12 may also be written as

$$R(t^*) = \frac{1}{2}\left[F_m(t^*) + F_m\left(t^* + \frac{2L}{c}\right)\right] + \frac{Mc}{2L}\left[v_m(t^*) - v_m\left(t^* + \frac{2L}{c}\right)\right] \quad \ldots\ldots (14)$$

It can be seen that the resistance calculation consists of the average of 2 force values selected at a time interval $2L/c$ apart, plus the average acceleration over the same time interval, times the pile mass. This expression reduces to Newton's Second Law as the interval $2L/c$ approaches zero (perfectly rigid pile).

Extension to Resistance Distribution Predictions

When the resistance distribution calculation by CAPWAP was presented (15), it was criticized as lacking uniqueness (16). The geotechnical engineer, accustomed to analyzing the results of static load tests where the source of the resistance forces is frequently desired, struggles with the problem of lack of uniqueness in the commonly used analyses. Intuitively, it has seemed that, with CAPWAP, the time of reflection of a

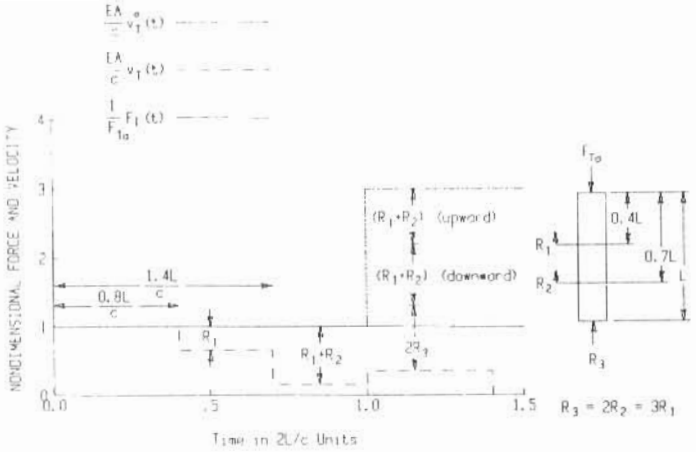

FIG. 3.—Pile Top Force and Velocity for Case with Several Resistance Forces

particular force should provide a unique solution. The derivation, previously given, makes it possible to prove that, in fact, the resistance distribution given by CAPWAP is unique within the assumptions contained in the derivation.

The effect of resistance forces at the pile head can be evaluated by examining force and velocity measurements at n different times, t_k, during the first $2L/c$ time period. Eq. 8 can be written in the form

$$F_m(t_k) - \frac{EA}{c} v_m(t_k) = \sum_{i=1}^{n} R_i H\left(t_k - 2\frac{x_i}{c}\right) \quad \ldots\ldots\ldots\ldots\ldots\ldots\ldots\ldots\ldots\ldots\ldots\ldots \quad (15)$$

for each time. A set of n simultaneous equations results with n unknown values of R_i. The values of F_m and v_m can be taken from the measurements. Solving these n equations leads to n, R_i values that are separated

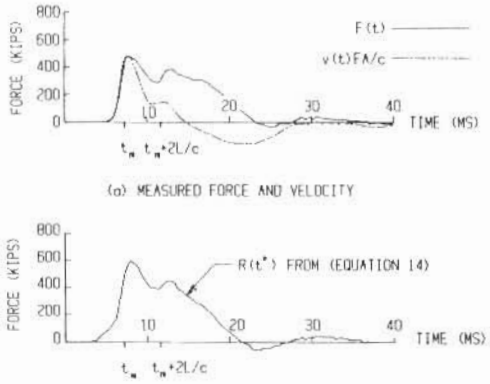

FIG. 4.—Resistance to Penetration from Eq. 14

by distances, $c(t_{k+1} - t_k)$. Conveniently, the t_k times can be chosen at constant time intervals, i.e., $t_{k+1} = t_k + \Delta t/c$ with $\Delta t = (L/c)/n$. Since there are n linear equations with n unknown R_i values, the solution of the equations is unique. Note that the toe force (R_3 in Fig. 3) must be determined by subtracting all skin friction forces from the total resistance, in accordance with Eq. 12. Thus, the uniqueness of the CAPWAP resistance distribution is proven under the assumption of an ideal plastic soil behavior.

For each $2L/c$ time interval of measured record, a theoretically unique set of n constants can be determined. From a practical point of view, only about $4L/c$ of the record can be analyzed since the measured signal will be too weak after that time interval (see Fig. 4).

Practical Considerations

Eq. 14 gives the total resistance to pile penetration. It was derived based on the assumption of a uniform pile cross section, linear elastic pile behavior, only axial stresses in the pile, and a rigid plastic soil resistance. The latter of these assumptions is of course not satisfied, nor is internal pile damping included.

Six different types of errors may arise:

1. Capacity is not fully mobilized at time $t^* + x/c$.
2. Impact energy is insufficient to activate all soil resistance forces.
3. The stress wave is short relative to the pile length over which resistance forces act; and resistance forces are, therefore, not maintained at full value during the time period considered.
4. Similar to error source 1, the toe resistance may not be fully mobilized at time $t^* + L/c$. Considering the soil model as elastic-plastic, as in wave equation work, this then is the case of large toe quake (8).
5. Some resistance is velocity dependent and must be subtracted to determine the static capacity.
6. The capacity can change due to setup or relaxation effects.

Error source 1 is usually avoided by choosing t^* at the time, t_m, i.e., when the first major velocity peak occurs. Fig. 4 shows that this is a reasonable choice in this particular example of a 38-ft (11.6-m) long HP 14 × 89 pile driven to limestone rock. The $R(t^*)$ curve has a maximum at time, t_m, which is interpreted as the pile's capacity. The later decrease of the $R(t^*)$ indicates that the pile rebounds. Actually, the derivation presented, using Heaviside functions which imply a perfectly plastic soil model, could have also been made using the elastic-plastic resistance law with quakes, i.e., pile displacement where soil elastic limit is reached, common in wave equation analysis (17). However, this would result in more complicated equations without adding to basic understanding. In general, the pile displacement at time, t_m, is similar to such commonly assumed wave equation quakes.

In cases where the hammer is small relative to the pile capacity, it is possible that the energy necessary to compress the soil to mobilize ul-

timate resistance is not available: Then, the capacity cannot be predicted. Thus, errors of type 2 cannot always be avoided. Fortunately, however, conservative predictions result and an obvious indication of such lower bound predictions is given by high blow counts [small permanent sets, usually less than 0.10 in. (2.5 mm)/blow]. This situation is similar to static proof testing with a jack that has a capacity less than the pile's ultimate resistance where the final net set is small.

For error case 3, a more complicated, though fortunately much less frequent situation occurs when an extremely high shaft resistance causes the pile head to rebound before time $2L/c$. An example is given in Fig. 5. Note the large difference between force and velocity developing shortly after impact. A negative (upward) velocity is induced before the pile toe effect becomes apparent at the pile head (time $t_m + 2L/c$).

In this example, the pile was a 10-in. (250-mm) diam pipe pile with a 5/8-in. (16-mm) wall thickness and a length of 145 ft (44 m). It was filled with concrete (c = 12.6 ft/ms) (3.8 m/ms) and dynamically tested after a waiting period (restruck). Due to a strong soil setup effect in the silty clays and silty sands, which created a large shaft resistance, the pile practically did not penetrate during restriking (blow count of 50 blows/in.). Again, as in the case of error source 2, the early rebound caused an underprediction in hard driving. Based on apparent shaft resistance from Eq. 15, however, an estimate of the underprediction is possible.

Fig. 6(*a*), showing force and velocity measurements on a 24-in. (600-mm) square concrete pile of 65 ft (20 m) length, shows error case 4. The soil consisted of silty sands and dense layers of clayey, silty sand near the pile toe. The records of force and velocity indicate very little shaft

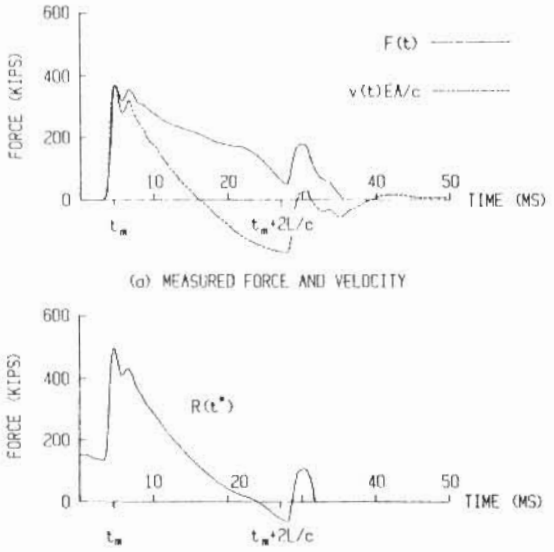

FIG. 5.—Resistance to Penetration for Very Large Skin Resistance

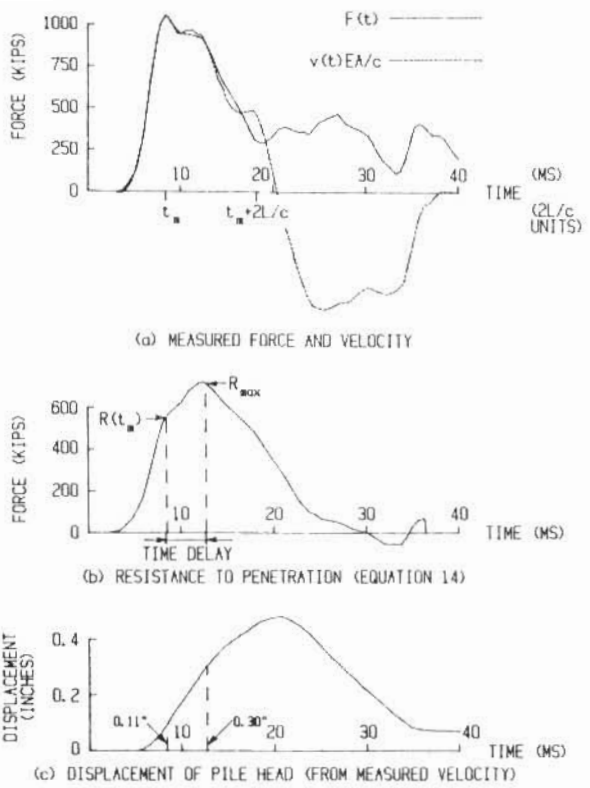

FIG. 6.—Resistance to Penetration for Tip Resistance with Large Quake

resistance (since they follow each other so closely) and an $R(t^*)$ curve, shown in Fig. 6(*b*), that increases significantly after time t_m. The displacement of the pile head, $d(t)$, given in Fig. 6(*c*) (obtained by double integration of the acceleration measurements), is only 0.11 in. (2.8 mm) at time, t_m, but 0.30 in. (7.6 mm) at time, t_m, plus 3.8 msec. Thus, by delaying the time of sampling a maximum capacity, R_{max} was found at a correspondingly higher toe displacement. Because of the relatively large size of the pile cross section, the necessary pile bottom compression was greater than the usually assumed 0.10 in. (2.5 mm). In some cases the displacement at maximum resistance has been found to be as large as 1 in. (25 mm) by CAPWAP analysis. This problem, known as large quake, is related to the soil characteristics (primarily in saturated soils) and the pile cross section (8).

Error source 5 indicates a more serious problem with Eq. 14. That is, while the forces resisting penetration are correctly determined, they may not represent the static soil capacity since some of the resistance arises due to the rapid penetration of the pile. An approach to dealing with this problem is to divide the total resistance to penetration into 2 parts: a static part, R_s, and a dynamic part, R_d. Thus, the total driving resistance is

$$R = R_s + R_d \quad \text{(16)}$$

Since the total resistance to penetration is known from Eq. 14, if R_d can be calculated, then R_s can be determined.

The assumption will be made that the dynamic resistance can be expressed as a linear function of the pile toe velocity. Thus

$$R_d = Jv_b \quad \text{(17)}$$

in which v_b = velocity of the pile toe; and J = the viscous damping constant (having units kip-sec/ft). A large volume of resistance distribution analyses by CAPWAP (12) has shown that the assumption of a damping resistance concentrated at the toe is reasonable. Thus, it is first necessary to determine toe velocity. For a free pile, the toe velocity is

$$v_b\left(t + \frac{L}{c}\right) = \frac{c}{EA} F_T(t) + v_T(t) \quad \text{(18)}$$

The change of toe velocity, induced by resistance forces, R_i, is

$$v_{b,i}(t) = -\frac{c}{EA} R_i \quad \text{(19)}$$

which is equally correct for shaft or toe resistance. The magnitude of toe velocity can now be obtained by subtracting the velocity reductions due to resistance from the free pile toe velocity, given in Eq. 18

$$v_b\left(t + \frac{L}{c}\right) = v_T(t) + \frac{c}{EA}\left[F_T(t) - \sum_{i=1}^{n} R_i\right] \quad \text{(20)}$$

If the damping force is proportional to toe velocity, using the expression of Eq. 17 and substituting into Eq. 16 gives

$$R_s = R(t^*) - J\left\{v_T(t) + \frac{c}{EA}\left[F_T(t) - \sum_{i=1}^{n} R_i\right]\right\} \quad \text{(21)}$$

in which R of Eq. 16 = total resistance to penetration given by Eq. 14. If the relationship of Eq. 11 is substituted into Eq. 21, and J is assumed proportional to EA/c by a damping constant j_c, then

$$R_s = R(t^*) - j_c\left[\frac{EA}{c} v_T(t^*) + F_T(t^*) - R(t^*)\right] \quad \text{(22)}$$

As was pointed out before, t^* is usually chosen at t_m. Furthermore, EA/c may be replaced by Mc/L, and the expression given by Eq. 14 substituted for $R(t^*)$.

$$R_s(t_m) = \frac{1}{2}(1 - j_c)\left[F(t_m) + \frac{Mc}{L} v_T(t_m)\right]$$

$$+ \frac{1}{2}(1 + j_c)\left[F\left(t_m + \frac{2L}{c}\right) - \frac{Mc}{L} v_T\left(t_m + \frac{2L}{c}\right)\right] \quad \text{(23)}$$

is obtained. $R_s(t_m)$ is the standard Case Method result. However, substituting t^* for t_m may lead to a larger static resistance value as previously mentioned.

An equally important consideration in the correlation of dynamic and static load testing is the effect of soil strength changes with time as in error source 6. Soils often exhibit substantial changes due to setup or relaxation effects. The effects of remolding, pore pressures, pile flutter or wobble creating an oversize hole, decrease with time. The dynamic testing methods presented here give the static capacity *at the time of testing*. Thus, to obtain a proper correlation with the static test, the pile should either be load tested as soon as possible after driving, or the pile should be restruck after a waiting period comparable to that given before starting the load test. Of course, to obtain the long term service load, restrike of the pile with the longest practical wait is always desirable. If dynamic methods are used at the end of driving and during several restrikes with varying wait times, the capacity can be thoroughly investigated as a function of time. Thus, errors of this type can be eliminated by testing during restrike.

Correlation

In Eq. 23, all of the quantities on the right side, except j_c, are known with measurements. At the time that this expression was derived, a large volume of data was available where dynamic measurements had been made on piles that had been statically load tested to failure. An empirical approach was used to extract values of j_c by substituting the static load test ultimate capacity for R_s and solving for j_c. Static load test ultimate capacities can vary widely for a given load test result depending on the failure definition used (1). This is particularly the case in coarse grained soils where a plunging failure is usually never fully achieved. The Davisson failure criteria (11) was selected. This approach was particularly attractive since it does not rely on the judgment of the evaluator.

Dynamic data were available on 69 test piles in which static load tests were carried to failure. Primarily, the data were obtained during a restrike: In a few cases where piles were driven in sand, the data were acquired at the end of driving. Of these piles, 41 were closed end pipes, 15 prestressed concrete, 10 timber and 3 H-piles. For each pile, a damping constant, j_c, was calculated, from Eq. 23, which produced a Case Method capacity equal to the statically observed value. In addition, a range of j_c values was determined so that a deviation from the static test value of not more than 20% resulted. Negative damping constants are physically meaningless so zero was the smallest value allowed. Fig. 7 shows a plot of the j_c range within 20% of the statically observed value. For piles with a capacity of less than 150 kips (660 kN), the accepted deviation range was increased to 30 kips (130 kN). This additional range in the acceptable damping constant value is indicated in Fig. 7 by the dashed lines. The load test data were organized according to the soil type in the region of the pile toe. It can be seen that the assumption of a damping constant dependent on soil type, as defined here, seems consistent with the available load test data.

Some cases should be explained further. It can be seen that in some examples, any value of damping constant between 0.0 and 2.0 will give results within 20% of the statically measured value. In these cases, near refusal conditions existed. Thus, the toe velocity during driving was near

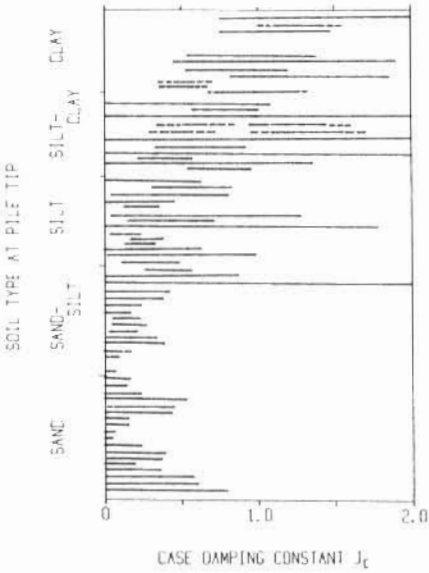

FIG. 7.—Damping Constant Determination by Correlation with Field Measurements

zero. If v_b = zero in Eq. 17, then the static capacity R_s, in Eq. 16, is equal to the total driving resistance, R, and is independent of or very insensitive to the selection of j_c. Conversely, in easy driving, the toe velocity will usually be high and, therefore, the capacity prediction becomes more sensitive to the selection of j_c.

Using the results presented in Fig. 7, recommendations can be made for ranges of j_c values. They are tabulated in Table 1. These recommendations were subjectively obtained by examining Fig. 7 and selecting a range such that a substantial portion of the data falls within the range. These values are tabulated in Table 1 in the column, "Suggested Range." It should be noted that the rather high values recommended for clay are to provide additional conservatism in a soil where less experience is available. In fact, one of the attractions of this approach is that conservatism can be added by the engineer by increasing the j_c value.

Single "best" values of j_c were selected for each soil type and are tabulated in the "Correlation Value" column of Table 1. These values were

TABLE 1.—Suggested Values for Clay

Soil type in bearing strata (1)	Suggested range, j_c (2)	Correlation value, j_c (3)
Sand	0.05–0.20	0.05
Silty sand or sandy silt	0.15–0.30	0.15
Silt	0.20–0.45	0.30
Silty clay and clayey silt	0.40–0.70	0.55
Clay	0.60–1.10	1.10

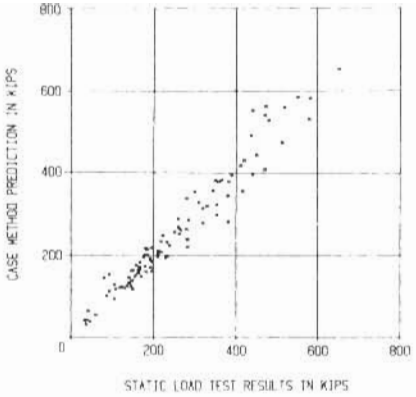

FIG. 8.—Case Method Capacity Compared with Static Load Test Results

then applied to the data of Fig. 7, and to subsequently obtained data in a correlation study shown in Fig. 8. The j_c values were obtained by examining the subsurface investigation information for the site. The results of Fig. 8, including 97 different sites, shows excellent agreement between Case Method and statically measured capacity. In fact, the difference is of about the same magnitude as the difference between different static load test evaluation procedures.

An example for a $j_c = 0.4$ is given in Fig. 9 together with the $j_c = 0.0$ solution. The pile was a 15 in. (380 mm) diam steel pipe, with a 1/2-in. (13-mm) wall thickness and a length of 80 ft (24 m). The soil in the bearing layer consisted of silty clays; and $j_c = 0.4$ is appropriate in such soils

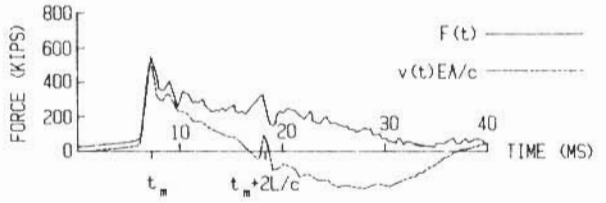

(a) MEASURED FORCE AND VELOCITY

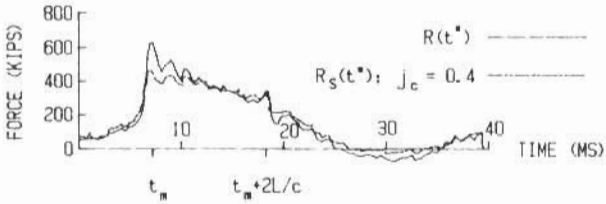

(b) RESISTANCE TO PENETRATION AND STATIC PREDICTION

FIG. 9.—Typical Example

as given in Table 1. Note that the static resistance value becomes independent of j_c if the bracketed term of Eq. 22 vanishes, i.e., where the two resistance curves in Fig. 9 intersect. Also, the $R_s(t^*)$ curve shows a relatively flat behavior which is reasonable for a static resistance, while the difference between $R(t^*)$ and $R_s(t^*)$ peaks at the time of highest velocity corresponding to the assumptions of viscous damping.

Conclusion

1. A method has been presented for calculating the resistance to penetration of a uniform cross section, elastic, driven pile from measurements of force and acceleration located below, but near the pile head.
2. The theoretical uniqueness of the CAPWAP resistance distribution has been proven within the limitation of an assumed ideal plastic soil behavior.
3. Limitations in the soil model used have been discussed and it has been shown that "large quake" soils can be identified and analyzed.
4. A method has been presented for static capacity determination using a velocity dependent resistance force. The damping constant is empirically determined and recommended values are given.
5. The dynamically determined static capacity correlates well with the statically measured result. Since the method gives capacity at the time of testing, testing is recommended to be performed on restrike to include soil strength changes due to setup or relaxation.
6. This method can be easily and practically applied in the understanding of pile driving.

Acknowledgments

The work reported here was completed during or was the outgrowth of a long term research project at Case Western Reserve University (previously Case Institute of Technology). This project was sponsored by the Ohio Department of Transportation and the Federal Highway Administration. Support was also obtained from several other state transportation organizations, equipment manufacturing companies, and pile driving contractors which are too numerous to mention.

The assistance of Ray Hanes, Leon Talbert, Ray Grover and Richard Dowalter, all employees or former employees of the Ohio Department of Transportation, was instrumental in the success of the project.

Appendix I.—References

1. Fellenius, B. H., "The Analysis of Results from Routine Pile Load Tests," *Ground Engineering*, Foundations Publications, Ltd., Vol. 13, No. 6, 1980, pp. 19–31.
2. Glanville, W. H., Grime, G., Fox, E. N., Davies, W. W., "An Investigation of the Stresses in Reinforced Concrete Piles during Driving," *Technical Paper No. 20*, British Building Research Station, London, England, 1938.
3. Goble, G. G., Kovacs, W. D., and Rausche, F., "Field Demonstration: Response of Instrumented Piles to Driving and Load Testing," *Proceedings of the Specialty Conference on Performance of Earth and Earth-Supported Structures*, Vol. III, Purdue University, Lafayette, Indiana, June, 1972.

4. Goble, G. G., Likins, G. E., and Rausche, F., "Bearing Capacity of Piles from Dynamic Measurements," *Final Report*, Department of Civil Engineering, Case Western Reserve Univ., Cleveland, Ohio, Mar., 1975.
5. Goble, G. G., Rausche, F., and Moses, F., "Dynamic Studies on the Bearing Capacity of Piles, Phase III," *Report No. 48*, Division of Solid Mechanics, Structures and Mechanical Design, Case Western Reserve University, Cleveland, Ohio, 1970.
6. Goble, G. G., Scanlan, R. H., and Tomko, J. J., "Dynamic Studies on the Bearing Capacity of Piles," Vols I and II, Case Institute of Technology, Cleveland, Ohio, July, 1967.
7. Goble, G. G., Tomko, J. J., Rausche, F., and Green, P. M., "Dynamic Studies on the Bearing Capacity of Piles, Phase II," *Report No. 31*, Vols. I and II, Division of Solid Mechanics, Structures and Mechanical Design, Case Western Reserve University, July, 1968.
8. Likins, G. E., "Pile Installation Difficulties in Soils with Large Quakes," Symposium on Dynamic Measurements of Piles and Piers, G. G. Goble, ed., ASCE Convention, Philadelphia, Pa., May, 1983.
9. Likins, G. E., "Field Measurements and the Pile Driving Analyzer," Proceedings of the 2nd International Conference on the Application of Stress Wave Theory on Piles, Stockholm, Sweden, May, 1984.
10. Michigan State Highway Commission, "A Performance Investigation of Pile Driving Hammers and Piles," *Final Report*, Lansing, Mich., Mar., 1965.
11. Peck, R. B., Hanson, W. E., and Thornburn, T. H., *Foundation Engineering*, 2nd ed., Wiley and Sons, New York, N.Y., 1974.
12. Rausche, F., "Soil Response from Dynamic Analysis and Measurements on Piles," thesis presented to the Case Western Reserve University, at Cleveland, Ohio, in 1970, in partial fulfillment of the requirements for the degree of Doctor of Philosophy.
13. Rausche, F., "Stress Wave Measuring in Practice," Theme Lecture and Paper for 2nd International Conference on the Application of Stress Wave Theory on Piles, Stockholm, Sweden, May, 1984.
14. Rausche, F., Goble, G. G., and Moses, F., "A New Testing Procedure for Axial Pile Strength," Third Annual Offshore Technology Conference, Paper No. OTC 1481, Houston, Tex., 1971.
15. Rausche, F., Moses, F., and Goble, G. G., "Soil Resistance Predictions from Pile Dynamics," *Journal of the Soil Mechanics and Foundations Division*, ASCE, Vol. 98, No. SM9, Proc. Paper 9220, Sept., 1972.
16. Screwvala, F. N., discussion of "Soil Resistance Predictions from Pile Dynamics," Rausche, F., Moses, F., and Goble, G. G., *Journal of the Soil Mechanics and Foundations Division*, ASCE, Vol. 98, No. SM9, Sept., 1972, Vol. 99, No. SM5, May, 1973.
17. Smith, E. A. L., "Pile Driving Analysis by the Wave Equation," *Journal of Soil Mechanics and Foundations*, ASCE, Vol. 86, Aug., 1960.
18. Timoshenko, S. P., and Goodier, J. N., *Theory of Elasticity*, 3rd ed., McGraw-Hill Book Company, New York, N.Y., 1970.

Appendix II.—Notation

The following symbols are used in this paper:

A = cross-sectional area of pile (or elastic rod);
c = velocity of wave propagation;
d = pile axial displacement;
E = modulus of elasticity;
F = axial pile force;
F_T = axial pile force at pile head;
F_{Ta} = applied axial force at pile head;

F_m = measured axial force;
J = viscous damping constant having units kip-sec/ft (N-sec/m);
j_c = case method damping constant $j_c = J\,c/EA$;
L = length of pile;
M = pile mass;
m = number of $2L/C$ time intervals after impact;
n = number of resistance forces;
R = total driving resistance;
R_i = ith pile resistance force;
R_d = dynamic portion of the resistance force;
R_s = static axial capacity;
t = time;
t^* = time used for starting computation of total driving resistance;
t_k = time interval for sampling force and velocity measurements;
t_m = time of first relative maximum in force and velocity measurement;
v = particle velocity in pile in axial direction;
v_b = particle velocity at pile toe;
$v_{b,i}^d$ = particle velocity at pile toe due to downward portion of wave from R_i;
v_c = particle velocity at pile head;
v_m = measured particle velocity;
v_R^c = particle velocity at pile head due to free pile case for resistance forces;
v_{1i}^d = particle velocity at pile head due to downward traveling wave from the resistance at ith location;
v_1^u = particle velocity at head of free pile;
v_{1i}^u = particle velocity at pile toe due to upward traveling wave from resistance at ith location;
x = variable defining the position along pile; and
ρ = mass density of pile.